Korean J. Chem. Eng., **27**(6), 1780-1785 (2010)
DOI: 10.1007/s11814-010-0408-z

A comparative study on the laser removal of Cs^+ ion from type 304 stainless steel

Hui-Jun Won†, Byambatseren Baigalmaa, Jei-Kwon Moon, Chong-Hun Jung, and Kune-Woo Lee

Korea Atomic Energy Research Institute, 1045 Daedeokdaero, Yuseong-gu, Daejeon 305-353, Korea
(*Received 10 August 2010 • accepted 23 August 2010*)

Abstract−A Q-switched Nd:YAG laser with a 1,064 nm and 450 mJ/pulse was employed to study the cleaning characteristics of Type 304 stainless steel specimens artificially contaminated with Cs^+ ions. Before laser irradiation, the specimens were treated with KCl and KNO_3, respectively. The relative atomic molar percent of Cs^+ ion on a metal surface was analyzed by EPMA. Before and after the laser irradiation, the morphology of the metal surfaces was investigated by SEM. The optimum laser fluence determined in the experimental range was 57.3 J/cm^2. For all the test specimens, more than 95% of the Cs^+ ions were removed by the application of 40 laser shots at 57.3 J/cm^2. Cs^+ ion removal efficiency was improved by the addition of nitrate ions to the contaminated metal surface. Surface temperature during the laser irradiation was calculated using Hertz-Knudsen equation to investigate the surface characteristics. A portion of particulates generated during the laser irradiation was found to accumulate around a crater of the specimen treated with the KCl solution. It was concluded that the ablated Cs^+ ions formed an oxide after thermal activation on the surface and deposited on a metal surface for the KCl system. The higher Cs^+ ion removal efficiency of the KNO_3 system was attributed to the decomposition of the nitrate ions at a relatively low temperature and the easy reaction of the Cs^+ ions with the oxygen generated from the decomposition of nitrate ions.

Key words: Laser, Cleaning, Cs^+, Nitrate, Chlorine, Hertz-Knudsen

INTRODUCTION

Cleaning by laser is a relatively recent technique for removing pollutants from surfaces that is currently finding various applications in many fields. A number of laboratory studies have focused on the possibilities of surface treatments such as removal of stain from ivory and related materials [1], cleaning of metal traces on circuit boards [2], investigation of surface morphology of single crystal [3], investigation of efficiency of concrete removal [4], and investigation of the effect of wavelength and the material removal mechanisms for removing copper oxide from copper [5]. The preparation of metal oxide films on the material by laser chemical vapor deposition was also reported [6].

Radioactive material is generated during the operation of a nuclear facility. Laser decontamination means the removal of radioactivity from the radioactively contaminated surface by the laser beam. Khalil et al. [7] presented an experimental and theoretical study of pulse laser ablation of stainless steel target. Various parameters such as laser power, pulse duration, enthalpy and heat capacity were used. The evaluation of software for the ablation processes was done. They reported that the ablation process induced by lasers is a collective phenomenon that basically involves two phenomena: the laser radiation-with matter interaction and the dynamic of the ablation plume. Kameo et al. [8] reported that the decontamination efficiency could be improved by employing an acid containing sodium silicate gel on to a contaminated metal surface before a laser application. To understand the role of laser irradiation on chemical reactions, chemical states of O and Fe in the oxide layer before and after decontamination were analyzed by X-ray photoelectron spectroscopy. They concluded that the contaminated layer was dissolved by the acid and combined with the gel under a laser irradiation condition. Rafique et al. [9] studied the XRD and SEM analysis of a laser irradiated cadmium. They used a pulsed Nd:YAG laser (10 mJ, 12 ns, 1,064 nm). From the test results, they reported that the hydrodynamic effects were apparent with a liquid flow which formed a recast material around the periphery of the laser focal area. Dimogerontakis et al. [10] studied the thermal oxidation induced during a laser cleaning of an aluminum-magnesium alloy. They used a Q-switched Nd : YAG laser unit with a pulse duration of 10 ns, and a wavelength of 1,064 nm. For the surface analyses of the treated samples, X-ray photoelectron spectroscopy (XPS) and secondary ion mass spectroscopy were used. They found that thermal oxidation took place on the alloy during the irradiation in air with a laser energy range from 0.6 to 1.4 J/cm^2. The feasibility tests to select a light source using surrogate specimens were performed [11]. The tested light sources were a continuous type CO_2 laser, a continuous type Nd : YAG laser and a pulse type Nd : YAG laser. It was found that the pulse type Nd : YAG laser was more efficient among them.

During the refurbishment of hot cells, decontamination work is necessary because it reduces the occupational exposure to workers and the burden for the safe management of radioactive wastes. Korean Atomic Energy Research Institute has operated the DFDF (DUPIC Fuel Development Facility) since 2000. All the DUPIC (Direct Use of PWR spent Fuel in CANDU) processes are executed in hot cells under a dry condition. As the operation age increases, the need to repair these hot cells increases. The radioactivity of the hot cells in the DFDF is presumed to be high and the predominant radionuclide is Cs-137. Also, the surface of a wall is contaminated with spent fuel particles. Before the refurbishment of the hot cells, the application of a remotely operated decontamination technique is required. The merits of a laser decontamination technique are a re-

†To whom correspondence should be addressed.
E-mail: nhjwon@kaeri.re.kr

mote application, a high decontamination factor, the generation of a small amount of secondary waste and a negligible occupational exposure to workers.

The objective of the study is to optimize the removal parameters of a Q-switched Nd : YAG laser system on the materials contaminated with Cs^+ ions. Especially, the effect of the chlorine and nitrate ions on the laser decontamination of the surrogate Type 304 stainless steel specimen was compared. To understand the reactions happening during the laser irradiation, the metal surface was analyzed by SEM, EPMA and XPS before and after a laser irradiation.

MATERIALS AND METHODS

Type 304 stainless steel specimens were used in the present experiment. The specimens were polished with abrasive papers. After they were washed with water and ethyl alcohol, they were dipped into an ultrasonic cleaner for 30 minutes to remove the remnants and dried. The specimens were contaminated with 0.015 M CsCl solution with injector and then dried again. They were treated with 0.03 M KNO_3 and 0.03 M KCl solutions, respectively. After drying, the specimen's surfaces were analyzed by SEM, EPMA and XPS. The relative atomic molar percent of the specimen's surface before a laser irradiation is listed in Table 1. As the concentration reveals the relative atomic molar ratio of elements on the metal surface, the composition Cs^+ ion is different among the chemical treatments. After a laser irradiation, the surface of the specimen was again analyzed.

Fig. 1 shows a schematic diagram of the experimental apparatus. The laser system emits a fundamental wavelength at 1,064 nm. Maximum pulse energy determined from the energy meter was 870 mJ/pulse. A pulse width of the Q-switched Nd : YAG laser determined from the oscilloscope was around 10 ns. All the tests were performed at the pulse energy of 450 mJ/pulse and the repetition rate of 10 Hz. Contaminated specimen was mounted on a stage that allowed the specimen holder to move by 25 mm in the X, Y and Z directions. An articulate mirror was used for the transfer and a convergence of a laser beam at a point on a target. The fluence was adjusted by turning the graduated knob of the torch attached to the articulate mirror. The specimen was irradiated by changing the number of laser shots.

Table 1. The relative atomic molar percent of a specimen surface before laser irradiation

Specimen \ Element	Cs	K	O	Cr	Fe	Ni	Others
CsCl+KCl	4.9	3.7	0.2	12.7	56.4	4.3	17.8
CsCl+KNO_3	5.6	3.2	3.9	18.6	59.0	3.4	6.3
CsCl	12.1	0.0	0.1	18.4	51.6	4.9	12.9

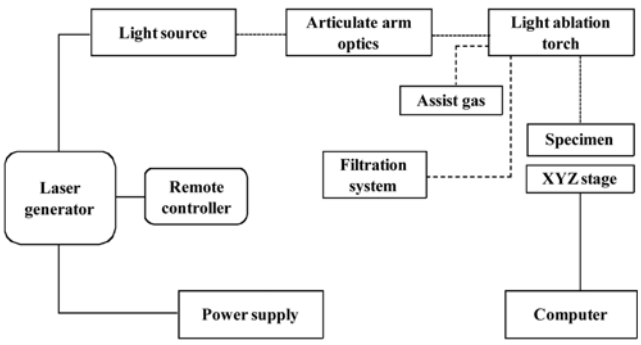

Fig. 1. Schematic diagram of the experimental apparatus.

RESULTS AND DISCUSSION

1. Cs^+ Ion Removal Characteristics

Cs^+ ion removal efficiency was measured as a function of the number of laser shots for 1,064 nm Q-switched Nd : YAG radiation of stainless steel specimen. Fig. 2 shows the remaining portion (C_s/C_o) of Cs^+ ion on Type 304 stainless steel specimens under various laser fluences. C_s and C_o are, respectively, the residual and initial relative atomic molar percent of Cs^+ ion. The remaining portion is decreased with the increase of the number of laser shots. For the 57.3 J/cm^2 and 229.3 J/cm^2 of laser fluence conditions, Cs^+ ion on the surface is drastically decreased during the first 10 shots. For the

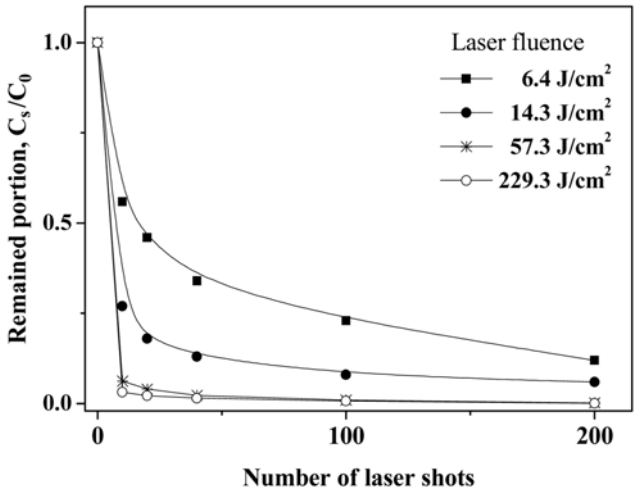

Fig. 2. Remaining portion of Cs^+ ion against the number of laser shots (0.015 M CsCl and 10 Hz).

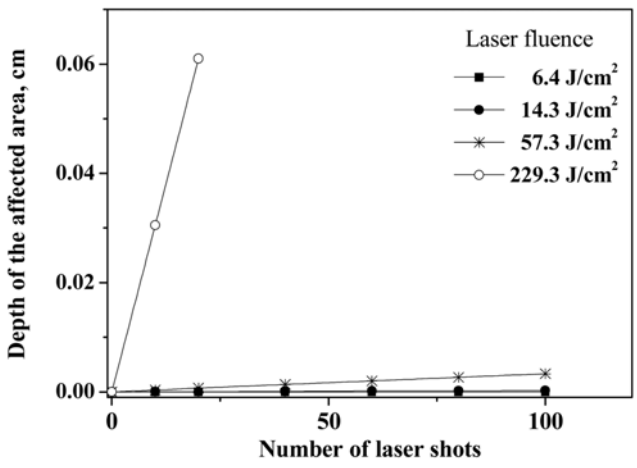

Fig. 3. Ablation of Type 304 stainless steel against the shot number under various fluences (1×10^{-3} atm and 10 Hz).

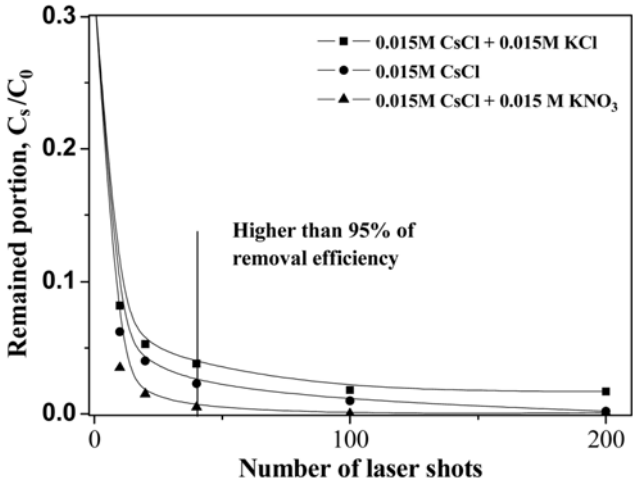

Fig. 4. Relationship between the Cs^+ ion removal efficiency and the number of laser shots (10 Hz and 57.3 J/cm^2).

6.4 J/cm^2 and 14.3 J/cm^2 of laser fluence conditions, however, Cs^+ ion on the surface is not so drastically decreased. For fluences higher than 6.4 J/cm^2, ablation plasma became clearly visible when the surface was irradiated.

The ablation rate of Type 304 stainless steel was measured against the number of laser shots under various fluence conditions and shown in Fig. 3. For the fluence conditions of 6.4 J/cm^2, 14.3 J/cm^2 and 57.3 J/cm^2, the ablation of Type 304 stainless steel is negligible. For the 229.3 J/cm^2 of laser fluence condition, ablation rate of Type 304 stainless steel is fast. This means that the ablation of Type 304 stainless steel occurred intensely and the generation of the secondary waste is not negligible at 229.3 J/cm^2 of laser fluence.

Consulting the test results of Figs. 2 and 3, it was determined that the optimum laser fluence for the removal of Cs^+ ion on Type 304 stainless steel is 57.3 J/cm^2.

Cs^+ ion removal efficiency was evaluated for the three kinds of contaminated solution by varying the number of laser shots at 57.3 J/cm^2. The remaining portion of Cs^+ ion against the number of laser shots is shown in Fig. 4. As shown, Cs^+ ion was easily removed by the Q-switched Nd : YAG laser for all the test specimens. More than 95% of Cs^+ ion was removed during the application of the first 40 laser shots (4 seconds). Contrary to the specimen treated with KNO_3 solution, more than 1% Cs^+ ion remained on the surface for the other two kinds of specimens. The specimen treated with KNO_3 solution shows better removal performance Cs^+ ion.

2. Surface Morphology during a Laser Irradiation

For the two kinds of specimens treated with KNO_3 solution and KCl solution, surface morphology was examined by SEM at a magnification of 100. SEM images of specimens before and after 20 and 40 laser shots are displayed in Fig. 5. The images show that the irradiated metal surface was melted, and it forms a crater by the laser irradiation. With the increase of the number of laser shots, the melting area affected by the laser irradiation is extended. For CsCl+KCl system, particulates are formed in the melting area.

It was reported that minute crystalline nuclei form at random points during the freezing of a molten material. These new nuclei then grow independently during the expansion of a surrounding matrix, because of the removal of the thermal energy [12]. Ablation can be based on a thermal activation only, on a direct bond breaking (photochemical ablation), or on a combination of these two work factors [13].

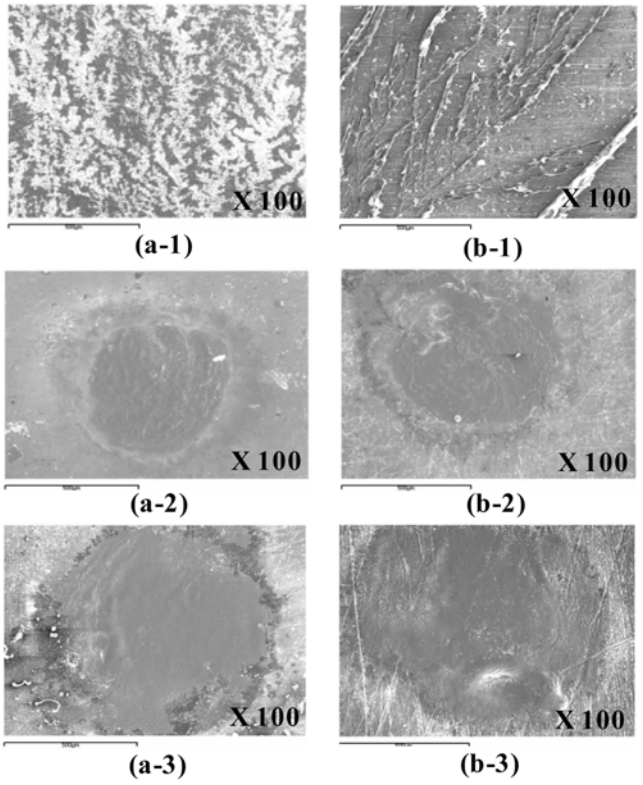

Fig. 5. SEM images of specimens before (1) and after irradiated 20 (2) and 40 laser shots (3), (a) 0.015 M CsCl+0.03 M KCl and (b) 0.015 M CsCl+0.03 M KNO_3.

Table 2. Representative values of type 304 stainless steel

Composition, wt%	Cr: 19.0
	Ni: 10.5
	Fe: 68.5
	Others: 2.0
Atomic weight, amu	Cr: 52.00
	Ni: 58.69
	Fe: 55.85
	Mn: 54.94
Specific gravity, g/cm^3	7.93

Ablation depth of Type 304 stainless steel at 14.3 J/cm^2 and 57.3 J/cm^2 in Fig. 3 was recalculated to the amount of the ablated of Type 304 stainless steel. The parameter values used for the calculation are listed in Table 2. The amount of Type 304 stainless steel per unit area was plotted against the laser irradiation time, and shown in Fig. 6. The slope at 14.3 J/cm^2 is 12.0 mole/cm^{2}s and at 57.3 J/cm^2 is 32.8 mole/cm^{2}s, respectively. The theoretical surface evaporation of solid at temperature T is given by the following Hertz-Knudsen equation:

$$J_i = s\frac{P_s(T) - P_i}{N(2\pi m_i k_B T)^{1/2}} \quad (1)$$

J_i is the mole flux of component i, s is the condensation coefficient,

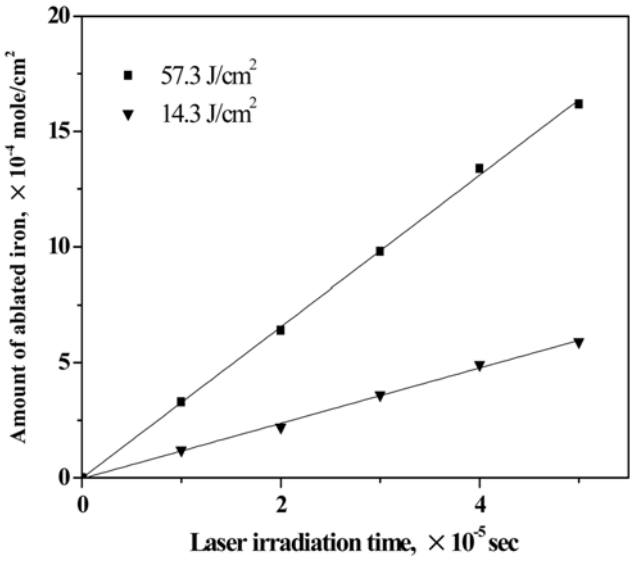

Fig. 6. Amount of ablated Type 304 stainless steel as a function of laser irradiation time.

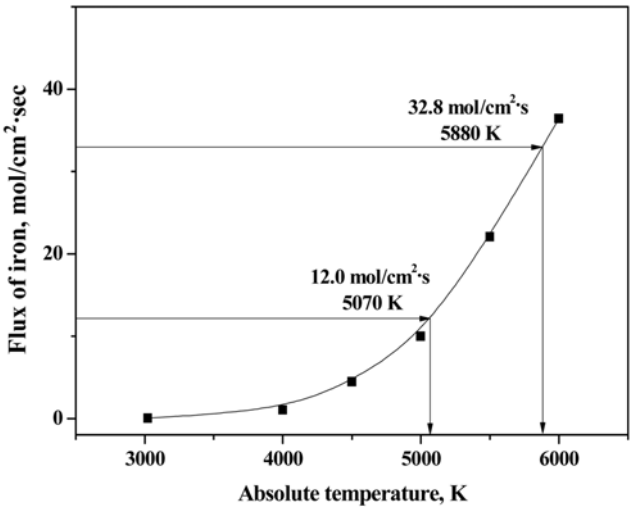

Fig. 7. Relationship between the theoretical iron flux and temperature.

$P_s(T)$ is the saturated vapor pressure, P_i is the partial pressure of vapor permanently present in the ambient, N is Avogadro's number, m_i is the atomic mass of component i, and k_B is the Boltzmann constant. The relationship between the temperature and saturated vapor pressure is described by the Clausius-Clapeyron relation:

$$\mathrm{Ln}\left(\frac{P_2}{P_1}\right) = -\frac{\Delta H_v}{R}\left(\frac{1}{T_2} - \frac{1}{T_1}\right) \quad (2)$$

P_1 is vapor pressure of iron at the boiling point, T_1 is the boiling point of iron, R is the gas constant, ΔH_v is the molar vaporization enthalpy of iron, and T_2 and P_2 are corresponding temperature and pressure at another point. By combining the two equations, the theoretical mole flux of iron can be calculated at a given temperature. The values used for the calculation are listed in Table 3. The theoretical flux of iron against the temperature was calculated and the relationship is shown in Fig. 7. Comparing Figs. 6 and 7, it was predicted that the surface temperature of Type 304 stainless steel during the laser irradiation was in the range from 5,070 to 5,880 K. Abdellatif et al. predicted that the temperature of plasma emitted from Al target at 1,064 nm was 18,700 K, and it increased gradually to reach 67,200 K at a distance of 500 mm from the target surface [14]. The surface temperature predicted in this study is much lower than the temperature of plasma. This can be ascribed to the heat loss on metal surface during the vaporization [15]. However, the experimental condition is sufficient to ablate the Type 304 stainless steel. The result also indicates that temperature jumping occurs only during the laser irradiation. The surface temperature returns to the room temperature during the time interval between the pulse laser irradiations. Considering the wavelength of the Nd : YAG laser is in the IR region of 1,064 nm and the calculation results, the ablation of the materials was predominantly caused by a thermal activation.

Table 3. Universal constants and parameters

J_i	$mol/cm^2 \cdot s$
s	0.5
P_i	1013.25 dyn/cm^2
N	6.022×10^{23} atom/mole
m_i	9.277×10^{-23} g/atom
k_B	1.381×10^{-16} erg/K·atom
R	8.314×10^7 J/mol·K
ΔH_v	3.496×10^5 J/mol
P_1	1 atm
T_1	3023 K

3. Surface Reaction during a Laser Irradiation

Most of contaminants on the surface were ablated by the thermal effect. However, the surface condition is different as shown in Fig. 5(a-3) and 5(b-3). The chemical states of surface atoms before and after irradiation of 20 laser shots on the Type 304 stainless steel were analyzed by XPS.

XPS spectra of specimen treated with CsCl+KCl solution are shown in Fig. 8. Peaks at 725 and at 740 eV correspond to Cs_{3d}. The peaks are not shifted with the irradiation of laser shots, but the area is decreased. The characteristics of Cs^+ ion on the surface did

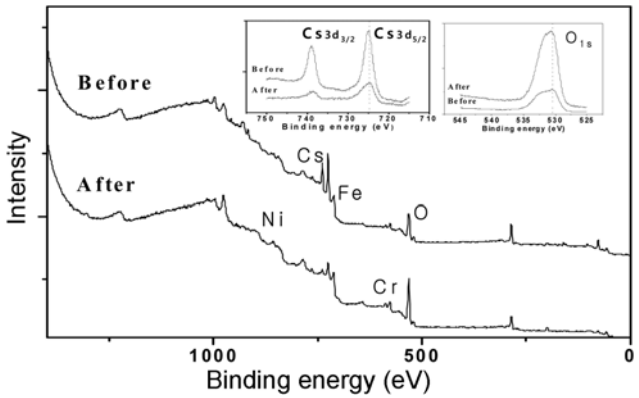

Fig. 8. XPS spectra of Type 304 stainless steel surface (0.015 M CsCl+0.03 M KCl) before and after 20 shots of laser irradiation.

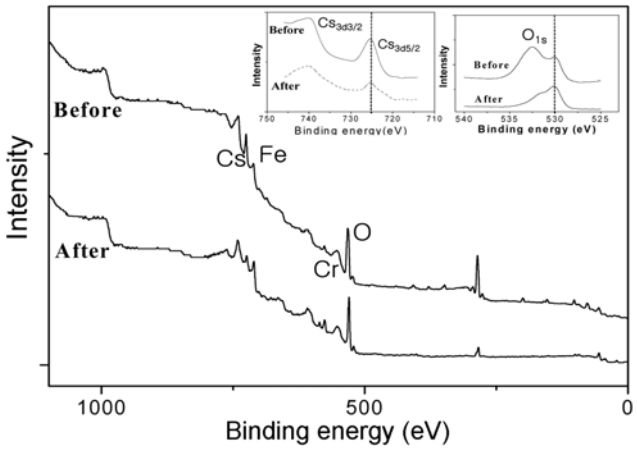

Fig. 9. XPS spectra of Type 304 stainless steel surface (0.015 M CsCl+0.03 M KNO_3) before and after 20 shots of laser irradiation.

not change during the laser irradiation. Peaks at 576.9 and 710.9 eV correspond to Cr and Fe, respectively. The peaks are shifted as the irradiation of laser shots. The XPS spectra of transition metal peaks have two peak maxima with binding energies, indicating the presence of metallic metal and metal oxide, respectively [16]. A peak at 530.3 eV which corresponds to O_{1s}, as shown in a small box of Fig. 8, grows as the irradiation of laser shots. It was reported that a peak at 530.3 eV corresponds to the oxygen in Fe_2O_3 [8]. Before laser irradiation, the oxygen peak at 530.3 eV came from slight surface oxidation of Type 304 stainless steel. Two explanations on the growth of oxygen peak are possible. First, the removal of contaminants increased the relative atomic molar percent of oxygen. Second, atmospheric oxygen reacted with the surface metal atoms during the laser irradiation.

Fig. 9 presents the XPS spectra recorded for the specimen surface treated with CsCl+KNO_3 solution before and after 20 shots of laser irradiation. After laser irradiation, the peak area of oxygen and cesium markedly decreased, but a peak area around 710.9 eV which corresponds to iron increased. Before laser irradiation, as shown in a small box of Fig. 9, the two peaks at 530.3 eV and 532.7 eV corresponding to O_{1s} are shown. The one near 532.7 eV, which corresponds to the nitrate oxygen disappearing after laser irradiation. After laser irradiation, a peak near 723.7 eV which corresponds to Cs_{3d} also significantly decreased and there is no peak shift.

From the investigation of XPS spectra, we could infer that the following reactions happened predominantly in the CsCl+KCl system during the laser irradiation. The boiling point of CsCl is 1,502 K and of KCl is 1,693 K, respectively.

$$\text{Thermal activation: } CsCl(sur) \rightarrow CsCl(g) \rightarrow Cs^{\ddagger}+Cl^{\ddagger} \quad (3)$$

$$KCl(sur) \rightarrow KCl(g) \rightarrow K^{\ddagger}+Cl^{\ddagger} \quad (4)$$

$$\text{Reaction near surface: } Cs^{\ddagger}+1/4\ O_2 \rightarrow 1/2\ Cs_2O(s) \quad (5)$$

$$K^{\ddagger}+1/4\ O_2 \rightarrow 1/2\ K_2O(s) \quad (6)$$

$$2\ Cl^{\ddagger} \rightarrow Cl_2(g) \quad (7)$$

Here ‡ is the reactive intermediate, (sur) is the surface, (g) is the gas state and (s) is the solid state. As illustrated in Fig. 5(a-3), $Cs_2O(s)$ particles formed near the metal surface deposited on the Type 304 stainless steel.

KNO_3 begins to decompose at 820 K [17] and it generates oxygen which can form an oxide with Cs^+ ion at a relatively low temperature. Contrary to the CsCl+KCl system, the predominant reactions happening in CsCl+KNO_3 system are inferred as the following:

$$\text{Thermal activation: } 2\ KNO_3(sur) \rightarrow 2\ N0_{2(g)}+K_2O_{(s)}+O^{\ddagger}(sur) \quad (8)$$

$$2\ CsCl(sur)+O^{\ddagger}(sur) \rightarrow Cs_2O(s)+2\ Cl^{\ddagger}(sur) \quad (9)$$

$$\text{Reaction near surface: } 2\ Cl^{\ddagger} \rightarrow Cl_2(g) \quad (10)$$

As illustrated in Fig. 5(b-3), $Cs_2O(s)$ and $K_2O_{(s)}$ particles formed on the surface are easily removed from the Type 304 stainless steel surface. The higher Cs^+ ion removal efficiency of CsCl+KNO_3 system is ascribed to the easy formation of $Cs_2O(s)$ particulates.

CONCLUSIONS

Cs^+ ion removal efficiency was optimized by varying the laser fluence and laser shot numbers. To obtain the high Cs^+ ion removal efficiency, the application time and the laser fluence should be increased or decreased according to the characteristic of the contaminated surface. The ablation rate of Type 304 stainless steel was fast at 229.3 J/cm^2 of laser fluence. The high ablation rate is caused by the high surface temperature and this affects the generation of the secondary waste. Considering the improvement of the removal efficiency, the specimen treated with KCl was more difficult to decontaminate than that with KNO_3. Cs^+ ions on the Type 304 stainless steel specimens were satisfactorily removed by the addition of nitrate ions with a little generation of the secondary waste. Application of a Q-switched Nd : YAG laser system for a decontamination of hot cell walls contaminated with radioactive cesium particles will be required to reduce the high radiation field before refurbishment or decommissioning. Finally, the present method also has a possibility to decontaminate the equipment in hot cells or to recycle the noble metals generated from nuclear facilities with little occupational exposure to workers.

ACKNOWLEDGEMENT

This work has been carried out under the Nuclear R & D Program funded by the Ministry of Education, Science and Technology.

REFERENCES

1. O. Madden, P. Pouli, M. Abraham and C. Fotakitos, *J. Cultural Heritage*, **4**(1), 98 (2003).
2. D. A. Wesner, M. Mertin, F. Lupp and E. W. Kreutz, *Appl. Surf. Sci.*, **96-98**, 479 (1996).
3. V. Cracium, N. Bassim, R. K. Singh, D. Cracium, J. Wermann and C. Boulmer-Lehorne, *Appl. Surf. Sci.*, **186**, 288 (2004).
4. M. Savina, Z. Xu, Y. Wang, C. Reed and M. Pellin, *J. Laser Appl.*, **12**, 1 (2000).
5. A. Kearns, C. Fischer, K. G. Watkins, M. Glasmacher, H. Kheyrandish, A. Brown, W. M. Steen and P. Beahan, *Appl. Surf. Sci.*, **127-129**, 773 (1998).
6. P. Zhao, A. Ito, R. Tu and T. Goto, *Appl. Surf. Sci.*, **256**(21), 6395

(2010).
7. A. A. I Khalil and N. Sreenivasan, *Laser Phys. Lett*., **2**(9), 445 (2005).
8. Y. Kameo, M. Nakashima and T. Hirabayash, *J. Nucl. Sci. Tech*., **41**, 919 (2004).
9. M. S. Rafique, M. Khaleeq-ur-Rahman, T. Firdos, K. Aslam, M. Shahbaz Anwar, M. Imran and H. Latif, *Laser Phys.*, **17**, 1138 (2007).
10. T. Dimogerontakis, R. Oltra and O. Heintz, *Appl. Phys. A*, **81**, 1173 (2005).
11. H. J. Won, C. J. Jung, J. K. Moon and C. H. Jung, *Proceedings Korean Rad. Waste Soc.*, **5**(2), 21 (2007).
12. C. R. E. Smallman and R. J. Bishop, *Modern physical metallurgy and material engineering*, Elsevier, Oxford, GB (2002).
13. J. C. Miller and Richard F. Haglund, *Ablation and Desorption*, Academic Press, San Diego, California, USA, **30** (1998).
14. G. Abdellatif and H. Imam, *Spectrochim. Acta*, **57**, 1155 (2002).
15. K. M. Song, Y. K. Hong, J. Yu and W. H. Hong, *Korean J. Chem. Eng*., **19**(2), 290 (2002).
16. D. Karthikeyan, N. Lingappan and B. Sivasankar, *Korean J. Chem. Eng*., **25**(5), 987 (2008).
17. C. M. Kramer, Z. A. Munir and J. V. Volponi, *Thermochim. Acta*, **55**, 11 (1982).